Identification of a biologically active fragment of ALK and LTK-Ligand 2 (augmentor-α)

Andrey V. Reshetnyak[a,1,2], Jyotidarsini Mohanty[a], Francisco Tomé[a], David E. Puleo[a], Alexander N. Plotnikov[a], Mansoor Ahmed[a], Navjot Kaur[b], Anton Poliakov[c], Arul M. Cinnaiyan[c], Irit Lax[a], and Joseph Schlessinger[a,1]

[a]Department of Pharmacology, Yale School of Medicine, New Haven, CT 06520; [b]Department of Neuroscience, Yale School of Medicine, New Haven, CT 06520; and [c]Michigan Center for Translational Pathology, University of Michigan, Ann Arbor, MI 48109

Contributed by Joseph Schlessinger, June 27, 2018 (sent for review May 8, 2018; reviewed by Sima Lev and William I. Weis)

Elucidating the physiological roles and modes of action of the recently discovered ligands (designated ALKAL1,2 or AUG-α,β) of the receptor tyrosine kinases Anaplastic Lymphoma Kinase (ALK) and Leukocyte Tyrosine Kinase (LTK) has been limited by difficulties in producing sufficient amounts of the two ligands and their poor stability. Here we describe procedures for expression and purification of AUG-α and a deletion mutant lacking the N-terminal variable region. Detailed biochemical characterization of AUG-α by mass spectrometry shows that the four conserved cysteines located in the augmentor domain (AD) form two intramolecular disulfide bridges while a fifth, primate-specific cysteine located in the N-terminal variable region mediates dimerization through formation of a disulfide bridge between two AUG-α molecules. In contrast to AUG-α, the capacity of AUG-α AD to undergo dimerization is strongly compromised. However, full-length AUG-α and the AUG-α AD deletion mutant stimulate similar tyrosine phosphorylation of cells expressing either ALK or LTK. Both AUG-α and AUG-α AD also stimulate a similar profile of MAP kinase response in L6 cells and colony formation in soft agar by autocrine stimulation of NIH 3T3 cells expressing ALK. Moreover, both AUG-α and AUG-α AD stimulate neuronal differentiation of human neuroblastoma NB1 and PC12 cells in a similar dose-dependent manner. Taken together, these experiments show that deletion of the N-terminal variable region minimally affects the activity of AUG-α toward LTK or ALK stimulation in cultured cells. Reduced dimerization might be compensated by high local concentration of AUG-α AD bound to ALK at the cell membrane and by potential ligand-induced receptor–receptor interactions.

cell signaling | cytokine | receptor tyrosine kinases | receptor activation | active fragment

Until recently, Anaplastic Lymphoma Kinase (ALK) and Leukocyte Tyrosine Kinase (LTK) receptors were known as "orphan" receptor tyrosine kinases (RTK) (1–3). The physiological ligands of ALK and LTK remained unknown for over two decades after these receptors were first discovered as oncogenic RTKs (4, 5). Importantly, several cancers were shown to be driven by gain-of-function mutations in ALK, including non-small-cell lung cancer and pediatric neuroblastoma, and drugs that block ALK activation have been successfully applied for treatment of ALK-driven cancers (6). Genetic studies have demonstrated that the proteins encoded by *Jeb* (Jelly belly) (7, 8) and *Hen-1* (Hesitation Behavior 1) (9, 10) function as activating ligands of ALK in *Drosophila melanogaster* and *Caenorhabditis elegans*, respectively. However, vertebrate homologs of either Jeb or Hen-1 proteins have not been identified.

The activating ligands of LTK were identified by screening a library of secreted and extracellular proteins for their ability to stimulate tyrosine phosphorylation of LTK (3). The identified ligands are gene products of unknown function designated FAM150A and FAM150B (family with sequence similarity) (11, 12). As both LTK and ALK share a highly conserved region in their extracellular domains, the two FAM proteins were subsequently tested for their ability to bind and activate ALK (13, 14). Designated as augmentor-β (AUG-β) or ALK and LTK-Ligand 1 (ALKAL1), FAM150A functions as a specific and potent ligand of LTK and a weak agonist of ALK (14). In contrast, FAM150B, also designated augmentor-α (AUG-α) or ALK and LTK-Ligand 2 (ALKAL2), functions as a potent activating ligand of both ALK and LTK (14). Two recent studies using zebrafish as a model system established a physiological link between augmentors/ALKAL1,2 with Ltk and demonstrated that, in zebrafish, these ligands are essential for iridophore development from neural crest cells and pigment progenitor cells (15, 16).

Sequence alignment of AUG-α and AUG-β from different species reveals two distinct regions: an N-terminal variable region and a conserved C-terminal augmentor domain (AD) (*SI Appendix*, Fig. S1) (14). In this report, we describe procedures for expression and purification of full-length human AUG-α and its truncated variant lacking the N-terminal variable region and consisting of only the AD. Using mass spectrometry, we map the disulfide bridges in human AUG-α and show that the four conserved cysteines located in the C-terminal AD form two intramolecular disulfide bridges, while a fifth nonconserved cysteine located in the N-terminal variable region is responsible for stabilizing a dimeric molecule via formation of an intermolecular disulfide bridge. We also demonstrate using mass spectrometry

Significance

The limited availability of the two ligands of the receptor tyrosine kinases ALK and LTK precluded the elucidation of their physiological roles and mechanism of action. In this report we describe two new approaches to produce full-length ALKAL2/AUG-α and an active variant lacking the N-terminal variable region. Detailed characterization of the primary structure and disulfide bridges using mass spectrometry demonstrates that the N-terminal variable region plays an important role in AUG-α dimerization and provides insight into the structural organization of a previously unknown augmentor fold. A variety of cellular experiments show that both AUG-α and its deletion mutant induce similar activation of ALK and LTK and stimulation neuronal differentiation of human neuroblastoma NB1 and rat pheochromocytoma PC12 cells.

Author contributions: A.V.R., D.E.P., I.L., and J.S. designed research; A.V.R., J.M., F.T., A.N.P., M.A., N.K., A.P., and I.L. performed research; A.V.R., J.M., F.T., D.E.P., A.N.P., M.A., N.K., A.P., A.M.C., I.L., and J.S. analyzed data; and A.V.R., D.E.P., I.L., and J.S. wrote the paper.

Reviewers: S.L., Weizmann Institute of Science; and W.I.W., Stanford University School of Medicine.

The authors declare no conflict of interest.

[1]To whom correspondence may be addressed. Email: andrey.reshetnyak@stjude.org or joseph.schlessinger@yale.edu.

[2]Present address: Department of Structural Biology, St. Jude Children's Research Hospital, Memphis, TN 38105.

This article contains supporting information online at www.pnas.org/lookup/suppl/doi:10.1073/pnas.1807881115/-/DCSupplemental.

Published online July 30, 2018.

that recombinant AUG-α expressed in mammalian cells does not contain posttranslational modifications. Finally, experiments are presented demonstrating that full-length AUG-α and a deletion mutant consisting of only the AD stimulate similar activation of cells expressing either ALK or LTK. Moreover, both full-length and the AUG-α deletion mutant stimulate neuronal differentiation of human neuroblastoma NB1 cells and PC12 (pheochromocytoma of rat adrenal medulla) cells in a similar dose-dependent manner. We conclude that deletion of the N-terminal variable region does not affect the activity or specificity of AUG-α toward LTK or ALK stimulation in cultured cells.

Results and Discussion

One of the key problems hampering investigation and establishment of the physiological roles and the mode of action of AUG-α and AUG-β is the difficulty of producing sufficient amounts of the two proteins to enable conducting such experiments. Our efforts to express and purify AUG-α and AUG-β using a variety of standard expression systems showed repeated low expression yields, poor solubility, and rapid degradation of both proteins. We have previously demonstrated that coexpression of AUG-α and AUG-β together with the ligand-binding domains of ALK and LTK, respectively, result in dramatic enhancement in expression of either AUG-α or AUG-β due to complex formation with ALK or LTK (14). While larger quantities of AUG-α and AUG-β can be produced by this coexpression method, this approach, ironically, is limited by the inability to efficiently dissociate the AUGs from the high-affinity ligand-receptor complexes, resulting in low yields of pure AUG-α and AUG-β proteins. Here, we describe a strategy to facilitate efficient dissociation of active AUG-α molecules from the complex with the ligand-binding region of ALK.

Both AUG-α and the ligand-binding region of ALK were expressed in the form of N-terminal Fc fusion proteins. To enable selective cleavage of the Fc moiety from AUG-α, a human rhinovirus 3C protease cleavage site was introduced into the linker region between the Fc portion and AUG-α. Furthermore, biotin acceptor peptides [also known as avi-tag (17)] were added to the N and C termini of the ALK fragment to enable site-specific biotinylation of the ALK receptor (Fig. 1*A*). To facilitate in vivo biotinylation of ALK, expression vectors of Fc-AUG-α and Fc-ALK were coexpressed in HEK 293 EBNA cells stably expressing the biotin ligase BirA. Fc-AUG-α in complex with Fc-ALK was first purified using protein-A affinity chromatography and was followed by digestion with 3C protease to remove the Fc moiety that is attached to AUG-α. The AUG-α molecules and the Fc-ALK were then immobilized onto NeutrAvidin beads through biotinylated ALK molecules. Finally, bound AUG-α was eluted from the NeutrAvidin beads using low-pH glycine buffer and immediately neutralized. Using this approach, we were able to produce a higher yield of full-length AUG-α (~1 mg/L, Fig. 1*B*). Notably, pure AUG-α preparations tend to precipitate in aqueous solutions at concentrations higher than 0.3 mg/mL. Moreover, the solubility of higher AUG-α concentrations can be improved upon addition of nondenaturing detergents and/or chaotropes.

After systematic search for additional expression systems, we found that fragments of the conserved AD of either AUG-α or AUG-β can be expressed in *Escherichia coli* as an N-terminal fusion with a histidine-tagged thioredoxin (Trx-tag) protein in the form of insoluble inclusion bodies (Fig. 1*A*). We next developed a refolding procedure for the conserved AD of AUG-α (designated AUG-α AD). Inclusion bodies were refolded, followed by affinity purification using nickel affinity chromatography and size exclusion chromatography to separate folded protein from misfolded aggregates. The Trx-tag was then cleaved via 3C protease digestion, and a soluble, correctly folded AUG-α AD was purified using cation exchange chromatography (Fig. 1*B*). While the tendency of AUG-α AD to aggregate is reduced compared with the tendency of full-size AUG-α to aggregate, AUG-α AD nevertheless also requires detergents or chaotropic agents to keep it in the solution and to prevent aggregation and precipitation. Therefore, determination of the dissociation constant of AUG-α AD using biophysical approaches such as size exclusion chromatography with multi-angle static light scattering (SEC-MALS) could not be reliably interpreted. However, these experiments demonstrated that dimerization of AUG-α AD is strongly compromised and that the majority of AUG-α AD exists as a monomer at micromolar concentrations.

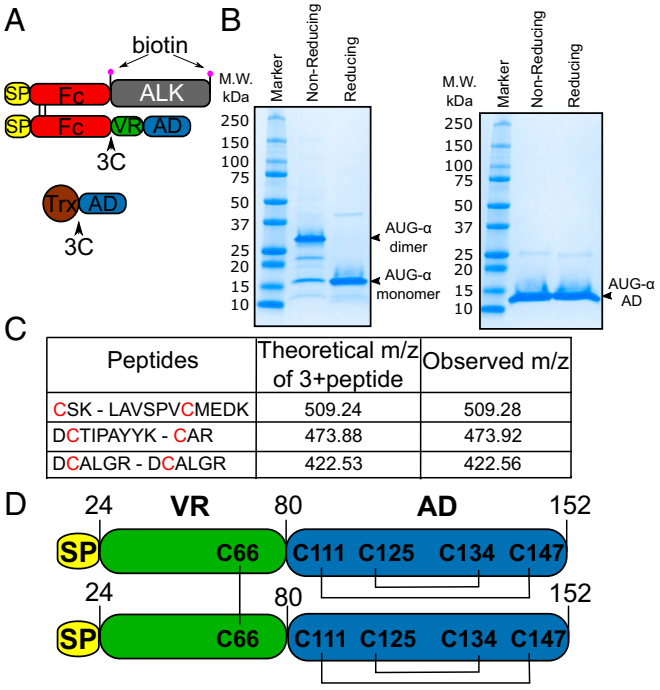

Peptides	Theoretical m/z of 3+peptide	Observed m/z
CSK - LAVSPVCMEDK	509.24	509.28
DCTIPAYYK - CAR	473.88	473.92
DCALGR - DCALGR	422.53	422.56

Fig. 1. AUG-α is expressed as a disulfide bridged dimer. (*A*) Schematic representation of expression constructs to produce full-length AUG-α from mammalian cells (*Upper*) or AUG-α AD from bacteria (*Lower*). Signal peptide is colored in yellow, Fc fragment in red, ALK fragment (residues 648–1030) in gray, AUG-α variable region (VR) in green, augmentor domain (AD) in blue, and Trx in brown. The 3C protease cleavage site is marked by an arrow, and the biotin acceptor peptides are marked by pink circles. (*B*) SDS/PAGE analysis of purified full-length AUG-α (*Left*) and a truncated version, AUG-α AD (*Right*), separated under nonreducing and reducing conditions as indicated in the upper panels. Molecular weight (M.W.) marker with corresponding molecular masses is shown on the left side of the gels. Under nonreducing conditions, full-length AUG-α migrates as a dimer, but migrates as a monomer upon reduction (as indicated on the right side). (*C*) Mass spectrometry mapping of disulfide bridges in AUG-α. Purified AUG-α was subjected to nonreducing SDS/PAGE, and the band corresponding to the dimeric form of AUG-α was excised, digested with trypsin, and used for mass spectrometry analysis. Disulfide-linked peptides are presented in the first column, and corresponding cysteines are highlighted in red. Theoretically predicted molecular masses for the corresponding 3+peptides are listed in the second column, and the observed *m/z* is listed in the last column. (*D*) Schematic representation of full-length AUG-α. Color code is the same as in *A* and *B*. Disulfide bridges are shown by black lines.

AUG-α Is Expressed in the Form of a Disulfide-Linked Homodimer. Sequence alignment of AUG-α and AUG-β from different species (*SI Appendix*, Fig. S1) shows that the two proteins contain four conserved cysteines in their C-terminal AD. Human AUG-α has an additional cysteine, Cys66, located in the N-terminal variable region. Interestingly, Cys66 of AUG-α is unique to primates and is replaced by either tyrosine or phenylalanine residues in other species (*SI Appendix*, Fig. S1). Since human AUG-α has an odd

BIOCHEMISTRY

number of cysteines, we hypothesized that the fifth cysteine residue may mediate disulfide-bridged homodimer formation. Indeed, purified AUG-α migrates in a nonreducing gel with an apparent molecular weight of 30 kDa, corresponding to migration of a dimeric protein, and in a reducing gel with an apparent molecular weight of 15 kDa, corresponding to an AUG-α monomer (Fig. 1*B*). In contrast, the AUG-α AD that is devoid of Cys66 migrates in nonreducing and reducing SDS gels with an apparent molecular weight of 13 kDa that corresponds to migration of a monomeric molecule (Fig. 1*B*). These experiments demonstrate that human AUG-α functions as a covalent dimer, linked by a disulfide bridge through Cys66.

To map the disulfide bridges of AUG-α, a protein band corresponding to the dimeric form of AUG-α was excised from a nonreducing gel, subjected to trypsin digestion, and analyzed by mass spectrometry. This analysis revealed that the four conserved cysteines in the C-terminal AD form intramolecular disulfide bonds, corresponding to one disulfide bridge between Cys111 and Cys147 and another disulfide between Cys125 and Cys134. The nonconserved Cys66 forms an intermolecular disulfide bond with the corresponding cysteine from another AUG-α protomer (Fig. 1*D*). The disulfide bridge organization of AUG-α is represented schematically in Fig. 1*D*.

Using N-terminal sequencing, we have confirmed that the native signal peptide of AUG-α is cleaved at the predicted position as determined using signalP (18) and that the mature protein starts at Gly25. Based on this analysis, mature AUG-α is composed of amino acids 25–152. Also, high accuracy electrospray ionization mass spectrometry determined that the molecular mass of recombinant AUG-α is 29,402 kDa, in perfect agreement with the theoretically predicted mass for dimeric AUG-α (MH1+ = 29,401 kDa; *SI Appendix*, Fig. S2). These results indicate that recombinant AUG-α expressed in human HEK 293E cells does not undergo posttranslational modification.

Extracellular Domain of ALK Contains a TNF-Like Motif. To gain insight into the organization of the ligand -binding region of ALK, a limited proteolysis of ALK (residues 648–1025) was conducted either alone or in complex with AUG-α AD (*SI Appendix*, Fig. S3 *A* and *B*). Experiments showed that trypsin, chymotrypsin, and subtilisin digestion produced several discrete, overlapping proteolytic ALK fragments while treatment with elastase, papain, or endoproteinase Glu-C left the majority of ALK intact (*SI Appendix*, Fig. S3*A*). Digestion with trypsin produced two major products corresponding to ∼16- and ∼22-kDa fragments, digestion with subtilisin produced two major products corresponding to ∼22- and ∼30-kDa fragments, and digestion with chymotrypsin produced a major product of ∼30 kDa (*SI Appendix*, Fig. S3). N-terminal peptide sequencing of the proteolytic digestion products excised from SDS/PAGE gels showed that the ∼22-kDa fragment corresponds to the glycine-rich region (GlyR) followed by the EGF-like motif (residues 809/810–1030). Interestingly, the ∼16-kDa fragment derived from trypsin digestion corresponding to residues Gln672 to Arg810 at the N terminus of the GlyR domain exhibits a weak homology to TNF-related apoptosis-inducing ligand and to other TNF-related proteins (19). This suggests that the extracellular domains of ALK and LTK contain a region with homology to a TNF-like motif (*SI Appendix*, Fig. S3*E*). The 30-kDa proteolytic fragments generated by subtilisin and chymotrypsin digestion correspond to the N-terminal peptides N-SISGYGAA-C and N-GYGAAGGK-C, respectively. These peptides are located in the middle of the predicted TNF-like motif, suggesting that the TNF-like motif may contain a flexible loop that is accessible for proteolytic cleavage. It is worth noting that complex formation with AUG-α AD did not affect formation of limited proteolysis products produced by trypsin, chymotrypsin, or subtilisin digestions, suggesting that these enzymes cleave ALK at regions distal from the AUG-binding site (*SI Appendix*, Fig. S3*B*). *SI Appendix*, Fig. S3*E*, represents an updated scheme for domain organization for ALK and LTK.

A Biologically Active Deletion Mutant Lacking the N-Terminal Variable Region of AUG-α. We next compared the activity of full-length AUG-α to the truncated AUG-α AD for the ability to stimulate ALK and LTK activation and cell proliferation mediated by ALK. In these experiments, NIH 3T3 cells stably expressing ALK or LTK were treated with increasing concentrations of full-length AUG-α or the AUG-α AD. Lysates from unstimulated or ligand-stimulated cells were subjected to immunoprecipitation with anti-ALK or anti-LTK antibodies followed by SDS/PAGE and immunoblotting with antiphosphotyrosine (pTyr) antibodies. As a control, blots were also probed with either anti-ALK or anti-LTK antibodies. The experiments presented in Fig. 2 *A* and *B* reveal a similar profile of tyrosine phosphorylation of ALK and LTK stimulation by either full-length AUG-α or AUG-α AD. These experiments show that the N-terminal variable region of AUG-α is dispensable for activation of ALK and LTK expressed in cultured cells.

We have previously demonstrated that coexpression of AUG-α together with ALK in NIH 3T3 cells results in autocrine stimulation of in vitro cell transformation (14). A doxycycline (Dox)-inducible system was used to express and compare the activities of full-length AUG-α and AUG-α AD using NIH 3T3 cells stably expressing

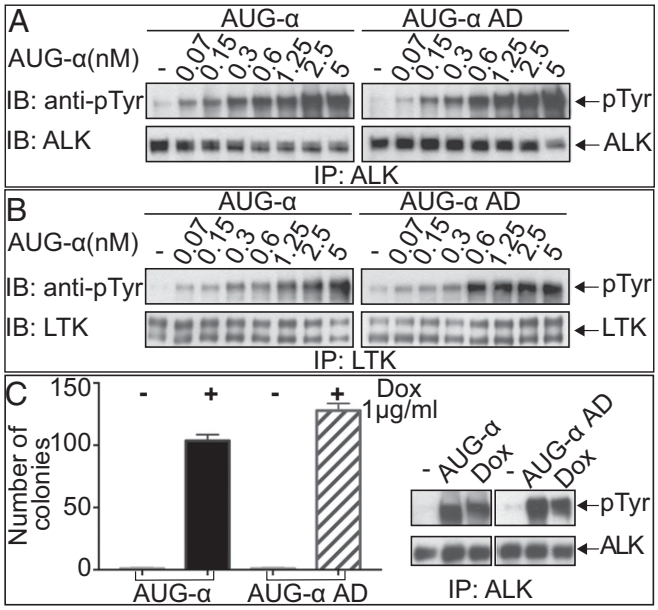

Fig. 2. Deletion of the N-terminal variable region of AUG-α does not affect kinase activity of ALK or LTK. (*A* and *B*) Immunoblot analysis of ALK (*A*) or LTK (*B*) autophosphorylation stimulated by different concentrations (as indicated) of purified AUG-α or AUG-α AD. NIH 3T3 cells stably expressing ALK or LTK were stimulated with increasing concentration of AUG-α or AUG-α AD for 10 min at 37 °C. Lysates of unstimulated or AUG-α–stimulated cells were subjected to immunoprecipitation (IP) using anti-ALK or anti-LTK antibodies followed by SDS/PAGE and immunoblotting (IB) with anti-pTyr (IB: pTyr) or anti-ALK or anti-LTK antibodies (as indicated). (*C*) NIH 3T3 cells were stably transfected with ALK and a Dox-inducible construct of AUG-α or AUG-α AD. (*Right*) Immunoblot analysis of ALK autophosphorylation stimulated by DMSO (indicated as by "−") and 50 μg of purified AUG-α or AUG-α AD, or Dox. (*Left*) Soft agar colony formation assay. Double-stable NIH 3T3 cells were treated with either DMSO or 1 μg/mL of Dox and grown in soft agar for 2 wk. Colonies were stained with crystal violet, counted, and plotted. Each experiment was performed in triplicate, and SD was calculated and plotted for each experiment.

ALK as previously described (14). The experiment presented in Fig. 2*C* shows that, upon Dox induction, full-length AUG-α or the AUG-α AD variant similarly stimulated ALK autophosphorylation and that ALK tyrosine phosphorylation is not stimulated in the absence of Dox induction. Moreover, Dox stimulation of NIH 3T3 cells expressing either full-length AUG-α or the AUG-α AD variant undergo similar cell transformation as revealed by colony formation in soft agar (Fig. 2*C*).

We next analyzed the time course of ALK and LTK activation in L6 cells stably expressing ALK or LTK. Specifically, we examined whether deletion of the N-terminal variable region of AUG-α may affect kinetics of ALK or LTK phosphorylation and whether it may change the mode of activation (sustained versus transient). L6 cells were stimulated with 10 nM of either full-length AUG-α or AUG-α AD, and receptor activation at different time points was assessed by immunoblotting (Fig. 3). Downstream phosphorylation of MAP kinase (MAPK) was also tested in the same experiment. The experiments presented in Fig. 4 reveal a similar profile of tyrosine phosphorylation of ALK and LTK as well as a similar MAPK response following AUG-α or AUG-α AD stimulation (Fig. 3). Taken together, these experiments demonstrate that the conserved AUG-α AD can potently and specifically stimulate ALK tyrosine phosphorylation, MAPK response, and transformation of cultured cells.

Neuronal Differentiation of PC12 Cells and NB1 Cells in Response to Stimulation with Full-Length or AUG-α Deletion Mutant. We next compared the ability of wild-type AUG-α and AUG-α AD to stimulate neuronal differentiation of PC12 cells ectopically expressing ALK. PC12 cells were derived from rat adrenal gland tumor and have been intensively applied as a model system for exploring neuronal differentiation induced by neurotrophic molecules and growth factors, such as nerve growth factor and the fibroblast growth factor family (20, 21). Here we demonstrate that both variants of AUG-α stimulate robust neurite outgrowth and promote differentiation of PC12 cells expressing ALK into differentiated neurons (Fig. 4 *A*–*E*).

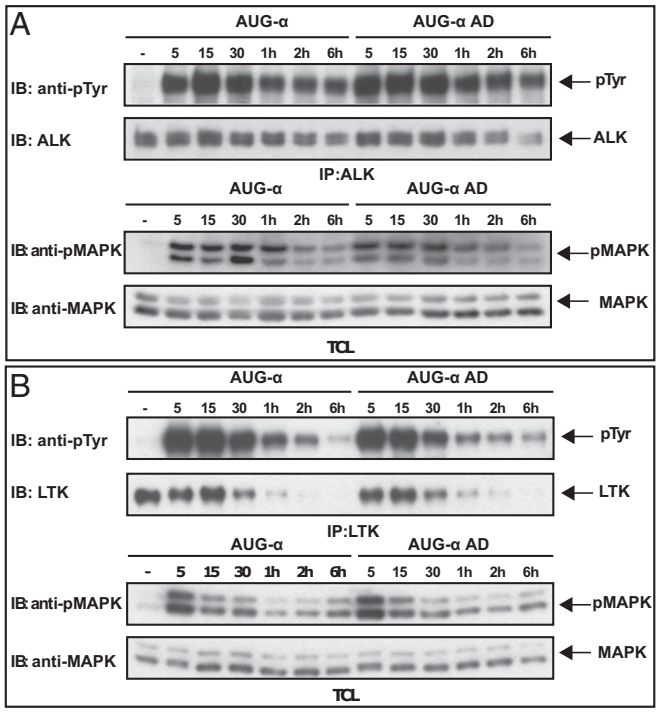

Fig. 3. Time courses of ALK and LTK receptor phosphorylation stimulated by AUG-α or AUG-α AD. Time courses of ALK (*A*) or LTK (*B*) phosphorylation in L6 cells stably expressing these receptors. Phosphorylation was induced by saturating levels (10 nM) of AUG-α or AUG-α AD. Cell lysates were subjected to immunoprecipitation (IP) by anti-ALK or anti-LTK antibodies, and phosphorylation was monitored by anti-pTyr antibodies (IB: anti-pTyr). Anti-ALK or anti-LTK antibodies were used as loading controls. Total cell lysates (TCL) and anti-phosphoMAPK or anti-MAPK antibodies were used to analyze MAPK phosphorylation in response to AUG-α or AUG-α AD stimulation at different time points.

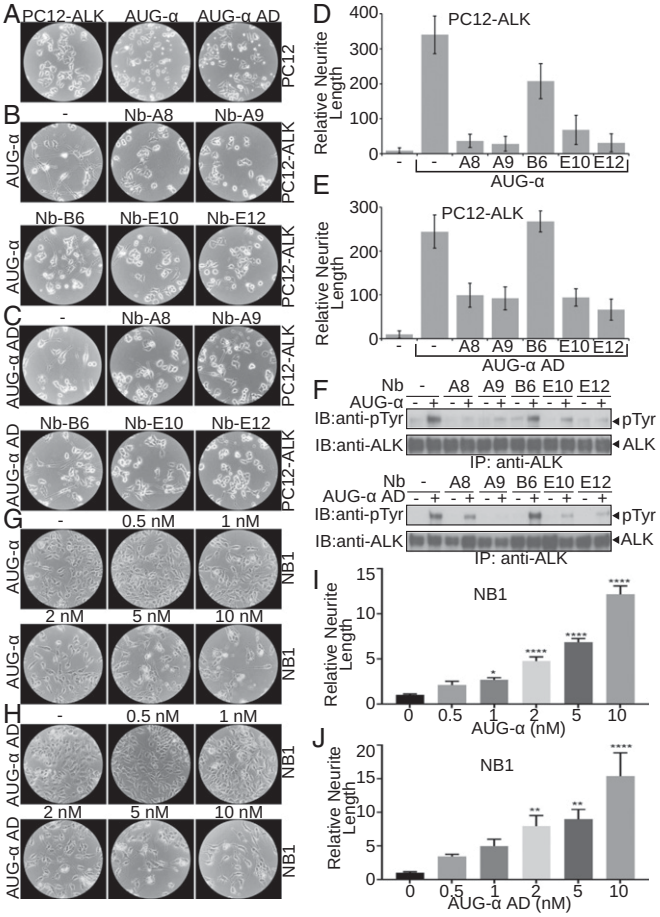

Fig. 4. AUG-α and AUG-α AD promote neurite outgrowth of neuronal PC12 and NB1 cells through ALK phosphorylation. (*A*–*F*) Neurite outgrowth of PC12 cells. (*A*) Unstimulated PC12 cells overexpressing ALK (*Left*). As a control, parental PC12 cells (two *Right* panels) were stimulated with 10 nM of AUG-α and AUG-α AD (as indicated). (*B* and *C*) PC12 cells overexpressing ALK were pretreated with 50 nM of anti-ALK nanobodies (A8, A9, B6, E10, and E12 as indicated) and were stimulated with 10 nM of either AUG-α (*B*) or AUG-α AD (*C*). (*D* and *E*) Relative neurite length per cell; values are means ± SEM; $n = 5$. (*F*) Inhibition of AUG-α (*Upper*) and AUG-α AD (*Lower*) stimulated ALK phosphorylation by nanobodies in PC12 cells assessed by immunoblotting (IB). (*G*–*J*) Neurite outgrowth of NB1 cells stimulated by AUG-α (*G* and *I*) or AUG-α AD (*H* and *J*). NB1 cells were assayed for neurite length with 0.0, 0.5, 1.0, 2.0, 5.0, and 10.0 nM concentration of AUG-α (*G* and *I*) or Aug-α AD (*H* and *J*). (*I* and *J*) Quantification of relative neurite length. Values are means ± SEM; $n = 6$. $^{*}P < 0.05$, $^{**}P < 0.01$, $^{****}P < 0.0001$, unpaired *t* test.

To address the role of ALK in mediating AUG-α stimulation of neurite outgrowth of PC12 cells, we generated and tested a panel of nanobodies [single Ig-like domain antibodies derived from llama (22)] that bind specifically to the extracellular domain of ALK and affect AUG-α–induced tyrosine phosphorylation of ALK (Fig. 4*F*). Nanobodies that inhibit AUG-α–induced ALK tyrosine phosphorylation (Nb-A8, Nb-A9, Nb-E10, and Nb-E12) were able to prevent neuronal differentiation of PC12 cells induced by either AUG-α or the AUG-α AD (Fig. 4 *B*–*E*). In

BIOCHEMISTRY

contrast, nanobody that binds to ALK and does not inhibit AUG-α–induced tyrosine phosphorylation of ALK (Nb-B6) did not influence neuronal differentiation of PC12 cells induced by either AUG-α or AUG-α AD (Fig. 4 *B–E*). These experiments demonstrate that AUG-α or AUG-α AD exhibit a similar ability to stimulate neuronal differentiation of PC12 and that ALK activation is necessary for AUG-α or AUG-α AD–induced neuronal differentiation of PC12 cells.

We also compared the ability of AUG-α or AUG-α AD to stimulate neuronal differentiation of NB1 neuroblastoma cells (derived from human tumor) that harbor high levels of endogenous ALK receptor. NB1 cells were treated with increasing concentrations of recombinant full-length AUG-α or AUG-α AD, and neurite outgrowth was assessed after 6 d of incubation. After several days, cells treated with both variants of AUG-α acquired characteristics of differentiated neurons (Fig. 4 *G–J*). At the same time, untreated cells or cells treated with lower concentrations (below 2 nM) of both variants of AUG-α maintained round morphology and did not display neurite extensions (Fig. 4 *G–J*).

Conclusions. While the receptor tyrosine kinases ALK and LTK have been known for several decades as oncogenic proteins, their physiological ligands were discovered only a few years ago (3, 13–16). Progress in elucidating the physiological roles and mode of action of ALK and LTK-Ligands 1 and 2 (ALKAL1,2, also designated AUG-β and AUG-α, respectively) was limited by availability of these ligands for in vitro and in vivo studies. In this report, we describe alternate approaches for expression and purification of a full-length AUG-α using a mammalian expression system and expression and purification of a truncated active fragment, AUG-α AD, by employing a bacterial expression system and a refolding procedure. Using these methodologies, we have overcome the low expression levels, poor stability, and rapid degradation of these ligands.

A detailed analysis of the primary structure of AUG-α using mass spectrometry revealed two intramolecular cysteine bridges connecting the four cysteines located in the conserved AD. On the other hand, the fifth cysteine residue, which is located in the variable region of AUG-α and is unique to primates, forms a disulfide bridge with the same cysteine of a second AUG-α molecule to stabilize formation of a covalent AUG-α dimer. The AD has a unique, unknown fold, which constitutes only ∼70 residues with four conserved cysteines stabilizing the 3D native conformation. Location and spacing between intramolecular disulfide bonds provide a structural signature of this specific protein fold. The AUG domain fold has an "enclosed" pattern of disulfide bridges (Cys111-Cys147 and Cys125-Cys134, Fig. 1*D*) with a 35-residue outer loop and an 8-residue inner loop size. Assignment of the AD intrachain disulfide bonds of the AUG domain highlights the structural information about this protein fold.

Comparison of cellular activities between full-length AUG-α and AUG-α AD reveals a similar stimulation of tyrosine phosphorylation and MAPK response induced in cells expressing either ALK or LTK. Moreover, both AUG-α and AUG-α AD exhibit similar profiles of ligand-induced ALK activation, MAPK response, and stimulation of neuronal differentiation of NB1 and PC12 cells, both with similar dose dependence. Experiments presented in this article show that the N-terminal region of AUG-α plays an important role in AUG-α dimer formation but is dispensable for ALK activation expressed in cultured cells.

Unfortunately, detailed analysis of the state of AUG-α or AUG-α AD dimerization, as well as quantitative ligand-binding analyses of cells harboring ALK or LTK, were challenging tasks, preventing interpretation of these experiments due to the tendency of AUG-α to aggregate. Thus, additional analysis must be performed to understand the role of the AUG variable region. Given that there is no difference in activation of cultured cells by full-length and AD AUGs, the variable region could be also involved in ligand localization and currently unknown functions. Preliminary biophysical experiments indicate that the dimerization of AUG-α AD is strongly compromised and that the majority of AUG-α AD exists as a monomer at micromolar concentration. It is therefore possible that the reduced capacity of AUG-α AD to dimerize is offset by high local concentration of AUG-α AD bound to ALK at the cell membrane and that ligand-induced dimerization of ALK is mediated in part by ligand-induced receptor–receptor interactions.

Materials and Methods

Expression and Purification of Full-Length AUG-α. Full-length AUG-α (residues 25–152) and the ligand-binding region of ALK (residues 648–1030) were cloned into pCEP4 vector in frame with IgG kappa signal peptide and human Fc domain at the 5′ end from AUG-α or ALK fragment. Flexible glycine serine linker $(GGGGS)_3$ and the 3C protease cleavage site (LEVLFQ/GP) were introduced between the Fc-tag and AUG-α. Biotin acceptor sequence (GLNDIFEAQKIEWHE) was introduced at 3′ and 5′ ends from the ALK gene. Full details about the Fc-AUG-α and Fc-ALK constructs are presented in *SI Appendix*.

To enable in vivo biotinylation of Fc-$ALK_{648–1030}$, HEK 293EBNA (293-E) cells were transfected with BirA enzyme using pLenti CMV Puro DEST vector and lentiviral infection protocol. Fc-AUG-α and Fc-$ALK_{648–1030}$ were coexpressed in 293-E-BirA cells using lipofectamine transient transfection in Opti-MEM media supplemented with 1 μM biotin. After transfection, the cells were incubated for 6 d. Media were then harvested and clarified, and the complex formed between Fc-AUG-α and Fc-$ALK_{648–1030}$ was purified by protein A Sepharose (Invitrogen) affinity chromatography. Purified complex was treated with 3C protease at a 1:100 weight:weight ratio at room temperature for 1 h. Cleavage reaction was monitored by SDS/PAGE. After 3C digestion, biotinylated ALK in complex with AUG-α was immobilized onto NeutrAvidin agarose beads (ThermoScientific). AUG-α protein was eluted from NeutrAvidin beads using elution buffer (100 mM glycine–HCl, pH 3.0, 0.1% CHAPS, 0.5 M urea) and immediately neutralized with 1 M Tris, pH 8.0, buffer.

Expression and Purification of AUG-α AD Deletion Mutant. A truncated variant of AUG-α (residues 77–152), lacking the N-terminal variable region (residues 25–76) and signal peptide (residues 1–24), designated AUG-α AD, was expressed using the pET expression system as a fusion protein with histidine-tagged thioredoxin A (Trx). A 3C protease cleavage site was introduced between the Trx and AUG domain of AUG-α. The protein sequence of the translated gene of Trx-AUG-α is presented in *SI Appendix*.

Trx-AUG-α AD fusion protein was expressed in the *E. coli* strain BL21-CodonPlus (DE3)-RIPL (Agilent). Cells were lysed, and inclusion bodies were solubilized in 6 M guanidine chloride and 10 mM DTT. Solubilized inclusion bodies were diluted in dilution buffer (2.6 M guanidine chloride, 500 mM arginine chloride, 50 mM Tris·HCl, pH 8.8, 10 mM reduced glutathione, 1 mM oxidized glutathione, 0.001% IGEPAL-CA630) up to a final concentration of 50 mg/L of total protein concentration. Diluted protein was dialyzed twice against dialysis buffer (10 mM Hepes, pH 7.4, 10% glycerol, 150 mM NaCl, 0.001% IGEPAL-CA630). After refolding, protein was purified by nickel affinity chromatography and size exclusion chromatography using HiLoad Superdex 200 16/60, equilibrated with 15 mM Hepes, pH 7.4, 500 mM NaCl, 0.5 M Urea, and 0.1% CHAPS. The Trx-tag was cleaved with 3C protease treatment at room temperature for 1 h at a 1:100 weight:weight ratio. AUG-α AD was separated from the cleaved Trx-tag using cation exchange chromatography. AUG-α AD was loaded onto a SourceS (GE Healthcare) column in 15 mM Hepes, pH 7.4, 150 mM NaCl, and 0.1% CHAPS buffer and eluted with linear NaCl gradient (0.15–1 M).

Cell Culture. NIH 3T3, L6, and PC12 cells stably expressing ALK or LTK were generated using a retroviral pBABE Puro expression vector as previously described (14). NIH 3T3 cells were cultured in the presence of DMEM containing 10% FBS, 100 U/mL of penicillin, 100 μg/mL streptomycin, and 1 μg/mL of puromycin. Cells were starved for 20 h in serum-free medium before stimulation for 10 min with indicated concentrations of either full-length AUG-α or AUG-α AD. Cell lysates were incubated with appropriate antibodies and protein A Sepharose (Invitrogen) overnight at 4 °C. The immunocomplexes were washed, boiled for 5 min with Laemmli sample buffer (BioRad), separated on SDS/PAGE, and then immunoblotted with anti-ALK, anti-LTK, or anti-pTyr antibodies.

Soft Agar Colony Formation Assay. Sequences encoding full-length AUG-α or AUG-α AD were cloned into a doxycycline-inducible pINDUCER vector (23). NIH 3T3 cells ectopically expressing ALK were used to generate cells with inducible variants of AUG-α. These cells were then plated at 5,000 cells per well in a six-well plate in 0.3% agar in the presence of DMSO as a control or 1 μg/mL doxycycline following 2 wk of incubation. Colonies were then stained with crystal violet and counted. Colonies from three replicate wells were quantified.

Neurite Outgrowth. PC12 cells were seeded in 10-cm plates at a relatively low density in DMEM containing 10% FBS, 10% heat-inactivated horse serum, 100 U/mL of penicillin, 100 μg/mL streptomycin, and 1 μg/mL of puromycin. The medium was supplemented with 50 nM of anti-ALK nanobodies and incubated in the presence of nanobodies where indicated. After 1 h of incubation at 37 °C, medium was additionally supplemented with full-length AUG-α, AUG-α AD, or buffer as a negative control. Cells were incubated at 37 °C and 5% CO_2, and images were acquired after 24 and 48 h. Neurite length was measured using NeuronJ in five replicates.

For NB1 neurite growth assay, four-well chamber slides (154917PK; ThermoScientific) were coated overnight with 10 μg/mL Laminin (23017-015; ThermoScientific). Approximately 2.5×10^4 NB1 cells/well were seeded with 0.0, 0.5, 1.0, 2.0, 5.0, and 10.0 nM concentration of AUG-α or AUGα AD in DMEM containing 4% FBS. Images were acquired after 6 d of seeding to measure neurite growth. Neurite length was measured using NeuronJ.

Mass Spectrometry. Full-length AUG-α was subjected to SDS/PAGE in nonreducing conditions. A protein band corresponding to a dimeric form of AUG-α was excised and digested with trypsin in gel for 2 h. The resulting peptides were extracted and analyzed using a Velos Pro mass spectrometer (ThermoScientific). As a control, after trypsin digestion, a peptide preparation was reduced with a 10-mM DTT treatment followed by identical mass spectrometry analysis.

N-Terminal Sequencing Methods. N-terminal sequencing was performed at Tufts University Core Facility.

Llama Immunization, Phage Display, and Nanobody Generation. Llama immunization, phage display selection, and nanobody production were performed according to previously published protocol (22). The complex of Fc-ALK with Fc-AUG-α was used for llama immunization using Gerbu adjuvant and a 6-wk immunization course. Llama immunization, isolation of peripheral blood mononuclear cells (PBMCs), and construction of a cDNA library from isolated PBMCs were performed at the Abcore Facility. ALK (residues 648–1030) was site-specifically biotinylated as described above and was used as an antigen for phage display selection. Individual nanobodies were expressed and purified as previously described (24).

ACKNOWLEDGMENTS. We thank members of the J.S. laboratory and Ewa Folta-Stogniew for productive conversations. This work was supported by NIH Grant 1S10OD018007. The SEC-MALS instrumentation was supported by NIH Award 1S10RR023748-01.

1. Lemke G (2015) Adopting ALK and LTK. *Proc Natl Acad Sci USA* 112:15783–15784.
2. Murray PB, et al. (2015) Heparin is an activating ligand of the orphan receptor tyrosine kinase ALK. *Sci Signal* 8:ra6.
3. Zhang H, et al. (2014) Deorphanization of the human leukocyte tyrosine kinase (LTK) receptor by a signaling screen of the extracellular proteome. *Proc Natl Acad Sci USA* 111:15741–15745.
4. Ben-Neriah Y, Bauskin AR (1988) Leukocytes express a novel gene encoding a putative transmembrane protein-kinase devoid of an extracellular domain. *Nature* 333: 672–676.
5. Morris SW, et al. (1994) Fusion of a kinase gene, ALK, to a nucleolar protein gene, NPM, in non-Hodgkin's lymphoma. *Science* 263:1281–1284.
6. Hallberg B, Palmer RH (2013) Mechanistic insight into ALK receptor tyrosine kinase in human cancer biology. *Nat Rev Cancer* 13:685–700.
7. Englund C, et al. (2003) Jeb signals through the Alk receptor tyrosine kinase to drive visceral muscle fusion. *Nature* 425:512–516.
8. Lee HH, Norris A, Weiss JB, Frasch M (2003) Jelly belly protein activates the receptor tyrosine kinase Alk to specify visceral muscle pioneers. *Nature* 425:507–512.
9. Ishihara T, et al. (2002) HEN-1, a secretory protein with an LDL receptor motif, regulates sensory integration and learning in Caenorhabditis elegans. *Cell* 109:639–649.
10. Reiner DJ, Ailion M, Thomas JH, Meyer BJ (2008) C. elegans anaplastic lymphoma kinase ortholog SCD-2 controls dauer formation by modulating TGF-beta signaling. *Curr Biol* 18:1101–1109.
11. Clark HF, et al. (2003) The secreted protein discovery initiative (SPDI), a large-scale effort to identify novel human secreted and transmembrane proteins: A bioinformatics assessment. *Genome Res* 13:2265–2270.
12. Strausberg RL, et al.; Mammalian Gene Collection Program Team (2002) Generation and initial analysis of more than 15,000 full-length human and mouse cDNA sequences. *Proc Natl Acad Sci USA* 99:16899–16903.
13. Guan J, et al. (2015) FAM150A and FAM150B are activating ligands for anaplastic lymphoma kinase. *eLife* 4:e09811.
14. Reshetnyak AV, et al. (2015) Augmentor α and β (FAM150) are ligands of the receptor tyrosine kinases ALK and LTK: Hierarchy and specificity of ligand-receptor interactions. *Proc Natl Acad Sci USA* 112:15862–15867.
15. Fadeev A, et al. (2018) ALKALs are in vivo ligands for ALK family receptor tyrosine kinases in the neural crest and derived cells. *Proc Natl Acad Sci USA* 115:E630–E638.
16. Mo ES, Cheng Q, Reshetnyak AV, Schlessinger J, Nicoli S (2017) Alk and Ltk ligands are essential for iridophore development in zebrafish mediated by the receptor tyrosine kinase Ltk. *Proc Natl Acad Sci USA* 114:12027–12032.
17. Beckett D, Kovaleva E, Schatz PJ (1999) A minimal peptide substrate in biotin holoenzyme synthetase-catalyzed biotinylation. *Protein Sci* 8:921–929.
18. Petersen TN, Brunak S, von Heijne G, Nielsen H (2011) SignalP 4.0: Discriminating signal peptides from transmembrane regions. *Nat Methods* 8:785–786.
19. Kelley LA, Mezulis S, Yates CM, Wass MN, Sternberg MJE (2015) The Phyre2 web portal for protein modeling, prediction and analysis. *Nat Protoc* 10:845–858.
20. Greene LA, Tischler AS (1976) Establishment of a noradrenergic clonal line of rat adrenal pheochromocytoma cells which respond to nerve growth factor. *Proc Natl Acad Sci USA* 73:2424–2428.
21. Togari A, Dickens G, Kuzuya H, Guroff G (1985) The effect of fibroblast growth factor on PC12 cells. *J Neurosci* 5:307–316.
22. Pardon E, et al. (2014) A general protocol for the generation of nanobodies for structural biology. *Nat Protoc* 9:674–693.
23. Meerbrey KL, et al. (2011) The pINDUCER lentiviral toolkit for inducible RNA interference in vitro and in vivo. *Proc Natl Acad Sci USA* 108:3665–3670.
24. Lee S, et al. (2018) Structures of β-klotho reveal a 'zip code'-like mechanism for endocrine FGF signalling. *Nature* 553:501–505.